International Journal of Applied Ceramic Technology
Ceramic Product Development and Commercialization

EFFECTS OF COMPOSITION AND FURNACE TEMPERATURE ON (Ni,Co)(Cr, Al)$_2$O$_4$ PIGMENTS SYNTHESIZED BY SOLUTION COMBUSTION ROUTE

Journal:	*International Journal of Applied Ceramic Technology*
Manuscript ID	ACT-4167.R1
Manuscript Type:	Article
Date Submitted by the Author:	n/a
Complete List of Authors:	Gilabert, Jessica; Instituto de Tecnologia Ceramica, Phisico-chemical characterization laboratory Palacios, Maria Dolores; Instituto Universitario de Tecnología Cerámica , Nanotechnology Sanz, Vicente; Universitat Jaume I, Instituto Universitario de Tecnología Cerámica; Universitat Jaume I, Chemical Engineering Mestre, Sergio; Universitat Jaume I, Instituto Universitario de Tecnología Cerámica; Universitat Jaume I, Ingeniería Química
Keywords:	combustion synthesis, pigment, spinels, microstructure

EFFECTS OF COMPOSITION AND FURNACE TEMPERATURE ON $(Ni,Co)(Cr, Al)_2O_4$ PIGMENTS SYNTHESIZED BY SOLUTION COMBUSTION ROUTE

J. Gilabert[a,*], M.D. Palacios[b], V. Sanz[b,c], S. Mestre[b,c]

[a]Instituto de Tecnología Cerámica. Asociación de Investigación de las Industrias Cerámicas. Castellón (Spain)

[b]Instituto Universitario de Tecnología Cerámica. Universitat Jaume I. Castellón (Spain)

[c]Departamento de Ingeniería Química. Universitat Jaume I. Castellón (Spain)

Abstract

The effects of composition and furnace temperature on $Ni_{1-\Psi}Co_{\Psi}Cr_{2-2\Psi}Al_{2\Psi}O_4$ ($0 \leq \Psi \leq 1$) pigments prepared by Solution Combustion Synthesis were studied. As-synthesized samples showed spinel-like spongy structure, very easy to grind. However, important differences on crystallinity, crystal size and microstructure were observed depending on composition and furnace temperature.

All pigments developed intense tones, covering a wide color palette because of composition influence, although little effect was observed with furnace temperature.

Stable crystalline structures, suitable grain size and high resistance against synthesizing variables and ceramic glazes make SCS pigments perfect candidates to be used in the ceramic ink-jet decoration.

Keywords: Combustion synthesis, pigment, spinels, microstructure

* Corresponding Author (jessica.gilabert@itc.uji.es)

The authors thank Universitat Jaume I for their support for the development of this research (Project Nr. P11B2015-04).

1 Introduction

The ceramic colorants sector is probably one of the most conservative areas in traditional ceramic manufacturing since almost every pigment and dye have been known for decades.[1] Pigments are colored crystals specifically designed for their dispersion in glazes or bodies, which must withstand physical and chemical attacks from the liquid phase formed during firing.[2]

The growing diffusion of ink-jet printing in the traditional ceramic sector implied a paradigm shift: the emphasis is moving from pigment (or dye) to ink.[3] Conventional micronized pigments proved to be unsuitable for digital decoration due to occlusion of nozzles, insufficient ink stability over time or low coloring power.[4,5] In order to overcome these drawbacks various strategies have been developed for traditional pigments as upgrading the manufacturing process by an expensive micronizing step. However, the high-energy milling can damage the pigment's crystalline structure and reduce its stability against chemical attack, decreasing the coloring power. In addition, optical properties change as function of particle size of pigments. Light absorption increases when pigment dimension decreases until a critical value. This phenomenon limits the gamut achievable with digital inks based on pigments synthesized by the traditional ceramic method. This circumstance is revitalizing the industrial interest towards alternative routes for pigment synthesis and technological solutions to improve the color performance. Co-precipitation method,[6,7] sol-gel route,[8,9] synthesis by using of polymeric precursors[10,11] or even reaction in molten salts[12] are some of them to highlight.

Solution combustion synthesis (SCS) is an effective method used worldwide for the synthesis of a variety of oxide materials in both nano and micro size interval.[13] In ceramic technology, this methodology has been used in the production of various ceramic powders for a variety of advanced applications. SCS method takes advantage of the energy resulting from the self-propagating highly exothermic redox reaction between a mixture of metal nitrates (oxidizers) and an optimal fuel (reducing agent). The ignition of the raw materials' solution is achieved by fast heating to relatively low temperatures, usually around 500 °C.[14] When synthesis conditions

are properly selected, the temperature reached in the reaction system (~ 1500°C) is high enough to allow direct formation of the desired compound without any additional heat treatment.

SCS method presents the inherent feature of obtaining foamy products, as a result of the generation of an enormous quantity of gases during combustion. When the stoichiometric solution of reagents is heated rapidly, it undergoes dehydration during the first 2 min. Later it decomposes with frothing as a result of the formation of the corresponding hydroxide gel of the ions involved with other products like urea nitrate, biuret, HNCO, and NH_3.[15] This mixture then foams due to the generation of gaseous decomposition products as intermediates, leading to enormous swelling. Reaction that decomposition products trigger because of their hypergolic characteristic in contact with each other, and leads to the generation of carbon dioxide, water vapor, nitrogen gas and ammoniac in important quantities.[16]

Many cases have been reported of successful application of SCS to obtain ceramic pigments,[17-19] and more concretely, to synthesize spinel structures.[20,21] Nevertheless, literature reports many cases of partial exploitation of combustion synthesis advantages due to the use of starting compositions and procedures that are not designed according to the desired product and targeted specifications.[14,20-24] Therefore, it is needed a better understanding and control of the parameters that can influence in SCS reaction, such as furnace temperature, atmosphere or initial composition.[25] The present paper is focused on the study of the influence of two important variables in the solution combustion synthesis process during the development of (Ni, Co)(Cr, $Al)_2O_4$ mixed spinels: initial composition and furnace temperature (T_0), which is related with the transference of the heat needed to ignite the mixture of raw materials. As reported in bibliography,[28-30] variations in the SCS parameters can cause a significant modification of the grain size and other microstructural characteristics of the final pigment. Therefore, having a suitable knowledge of the composition and furnace temperature effects, based on the resulting powder characteristics point of view, is one of this research's objectives.

Extreme spinels selected, $CoAl_2O_4$ and $NiCr_2O_4$, are two of the most important spinel-type pigments used in ceramic sector and cover a wide color palette from a deep blue, also known as Thenard's blue,[31] to an intense green.[32]

2 Experimental procedure

The development of $Ni_{1-\Psi}Co_{\Psi}Cr_{2-2\Psi}Al_{2\Psi}O_4$ pigment by SCS required the preparation of suitable stoichiometric aqueous solutions of the corresponding nitrates and urea (all reactants used were from Panreac Química, S.A.U. Spain), according to the following chemical equation.

$$6(1-\Psi)Ni(NO_3)_2 + 6\Psi Co(NO_3)_2 + 12(1-\Psi)Cr(NO_3)_3 + 12\Psi Al(NO_3)_2 + 40CH_4N_2O \rightarrow 6Ni_{1-\psi}Co_{\psi}Cr_{2-2\psi}Al_{2\psi}O4 + 64N_2 + 40CO_2 + 80H_2O \ (\sim 31 \text{ mol of gases/mol spinel}) \quad [1]$$

The solutions varied the proportions of nickel, cobalt, chromium and aluminium nitrates covering the range $0 \leq \Psi \leq 1$ in steps of 0.2. Table I shows initial solution compositions used in each test carried out in the present study. Fuel/oxidizer ratio was maintained constant to limit the number of variables in the study.

Prepared solutions were magnetically stirred during 30 min to assure perfect dissolution of salts. In every experiment, solution was prepared in a glass container and transferred to a stainless steel container immediately before its insertion in a preheated kiln at the selected furnace temperature (BLF 1800, Carbolite Furnaces Ltd, UK), where it remained during 20 min of soaking time. Each pigment was synthesized thrice modifying the furnace temperature (T_0) in every one (400ºC, 500ºC and 600ºC). Selected temperatures ranged around the most suggested point in literature,[14,33] in order to determine the optimal T_0 value for every spinel.

As-synthesized pigments were milled in agate jar ball mills with water (Pulverisette 5, Fritsch GmbH, Germany). Then, pigments were dried under infrared lamps and sieved through a 200-µm mesh to completely disaggregate the particles.

Characterization of pigments was carried out using different techniques. An energy-dispersive X-ray microanalysis instrument (Genesis 7000 SUTW, EDAX, USA) coupled to an FEG-SEM

(QUANTA 200F, FEI Co, USA) was selected to determine chemical composition and microstructure respectively. Specific surface area values were determined according to the BET method (Brunauer-Emmet-Teller) using nitrogen gas as adsorbate (Tristar 3000, Micromeritics, USA) and a degassing temperature of 150ºC for 3 hour. Identification of crystalline phases and crystallinity measurements was carried out by means of a XRD (Theta-Theta D8 Advance, Bruker, Germany), with CuK radiation (λ = 1.54183 Å). The generator applied an intensity light source of 45 kV and 40 mA. XRD data were collected in a 2θ interval from 5º to 90º with a step width of 0.015º and a counting time of 1.2 s/step by means of a VÅNTEC-1 detector. Raw data were refined by Rietveld method using 4.2 version of the Rietveld analysis program DIFFRACplus TOPAS. A pseudo-Voight function to describe peak shapes was assumed. The refinement protocol included the background, the scale factors and the global-instrument, lattice, profile and texture parameters. Rwp (Weight profile R-factor) and GOF (Goodness of fit) parameters were obtained to evaluate the quality of the refinement. Thermogravimetric analyses using a TGA-SDTA (851E/160, Mettler Toledo, Switzerland) were conducted in a platinum vessel from 25 ºC to 1000 ºC at 10 ºC/min of heating rate using a dynamic air atmosphere (50 mL/min flow).

Pigments were added to a transparent single-fired porous tile glaze in a 2/98 proportion in weight for evaluating their coloring power (chemical composition in wt% of oxides 0.5% Na_2O 4.0 % K_2O, 15.3% CaO, 0.9 MgO, 9.0% ZnO, 7.4% Al_2O_3, 3.0% B_2O_3, 59.5% SiO_2). The glazed tiles were fired in an electric laboratory kiln at maximum temperature 1100 ºC and 6 min of soaking time. A spectrophotometer (Color Eye 7000A, X-Rite Inc, USA), was used to measure the reflectance curves of the glazes. CIELab* chromatic coordinates were calculated using CIE Illuminant D65 and CIE 10º standard observer.

3 Results and discussion

All as-synthesized pigments presented a highly spongy aspect with very low bulk density (Fig.1), justified by the large volume of gases generated during SCS reaction. These gases are responsible for the increase of the final product volume. Nevertheless, the morphology was not

the same in all cases but it substantially changed with composition. As Co^{2+} and Al^{3+} content increased ($\Psi > 0$), the pigments evolved from occupying the whole volume of the reaction container (10 times larger than the volume of the initial solution), to practically be maintained as a lightly spongy coating on the bottom of the container (id est, similar to the initial solution volume). This fact indicated that the spongy effect was more pronounced when Ni^{2+} and Cr^{3+} ions were involved in the synthesis. Moreover, the observed effect was even more strengthened as the furnace temperature increased. As a hypothesis, these morphological differences could be related with urea decomposition around 80ºC, which generates OH^- ions. Therefore, the increase of pH can provoke the precipitation of hydroxides. In the case of $Ni(OH)_2$ and $Cr(OH)_3$, they were more gelatinous and, therefore, they retain more solution, which favors the foaming process under the pressure of steam first, and combustion products after. In the case of $Co(OH)_2$ and $Al(OH)_3$, they were less gelatinous, retain less water, and the expansion under the generated gases was lower. Under this hypothesis, a higher furnace temperature accelerates the heat transfer between the kiln and the solution, allowing that the time difference between hydroxides precipitation and steam generation was shorter. In consequence, more water was retained and the foaming effect of steam increased.

The consequences of foaming degree over the microstructure were studied by means of SEM. A relation was observed between the spongy aspect and the grain characteristics. Fig. 2 shows the evolution of pigment's grain morphology and size as function of composition and T_0. According to the images, grain sizes were higher while composition was richer in Ni^{2+} and Cr^{3+}, because of the best reaction effectiveness of SCS with this ion composition. The effect was even more pronounced in the samples with $\Psi = 0.0$, which showed the highest grain size with a very angular-shape morphology, which approaches in some cases to the theoretical crystalline habit of spinel.[34] The grain size in $NiCr_2O_4$ samples showed a broad size distribution since grains from 20 to 100 nm approximately were found during analysis. On the other hand, when Co^{2+} and Al^{3+} ion content increased progressively, the grain size decreased and their shape appeared to be more rounded.

With respect to T_0 effect, it is evident that higher temperatures favored the development of larger grain sizes. However, this phenomenon is more evident for the mixed spinels. By contrast, the effect for spinels with extreme compositions (Ψ = 0.0 or 1.0), although perceptible, is subtler. In consequence, furnace temperature is a variable to be controlled because it can induce important modifications in pigment's grain size. Mainly, when composition by itself works towards the opposite direction.

A more general view of the evolution of microstructure with composition and furnace temperature was obtained by measuring specific surface area of pigments (Table II).[14,25,35] Results showed an exponential-like trend in specific surface area with Ψ. Furnace temperature increase yielded a decrease in specific surface, also obvious and more pronounced as Ψ increased. This trend leads to the supposition that there is an intergrain porosity, which is favored as spinels are enriched in cobalt and aluminum, because the grains are smaller and probably less sintered. The T_0 effect can be interpreted as the effect of an incipient sintering of the grains during the 20 minutes of soaking time employed in the synthesis, which must be more intense at higher temperatures.

Pigment chemical composition measured by EDX (Fig. 3) showed a good correlation with the theoretical atomic composition. In previous published reports about solid solution spinels, a good correlation between experimental and theoretical values was demonstrated in all compositional range.[36] For that reason, not all compositions developed in this study have been analyzed by EDX, only the most representatives for the research. All results obtained indicated that SCS is a method to consider for developing pigments with chemical composition very similar to the theoretical target.

XRD analysis showed that all pigments presented the same spinel-type Fd-3m crystal structure (face-centered). As an example, Fig. 4 shows the complete diffraction patterns for all composition range of $(Ni,Co,)(Cr,Al)_2O_4$ samples synthesized at T_0=500ºC. However, great differences in crystallinity were detected as function of composition and T_0 (Fig. 5). In addition, no traces of non-reacted oxides or other secondary products were identified in the patterns.

I_{100} reflection's intensity of spinel presented a decreasing trend as the structure was being enriched in Co and Al (Ψ increased), evolving from a well-defined pattern to a practically amorphous hallo with very low crystallinity. The evolution was progressive and no evidence of inflexion points were observed. In consequence, it can be said that high contents of Ni^{2+} and Cr^{3+} favors the rearrangement of ions into the spinel network during the SCS reaction while Co^{2+} and Al^{3+} presence reduces crystallization capability of the system. In other words, the compositions with Ψ next to or equal to 1.0 seemed to work against spinel structure development. In those cases, SCS does not allow ions to rearrange adequately to a full-crystallized spinel. Possibly SCS fast kinetics makes the Co^{2+} and Al^{3+} rearrangement difficult as it was suggested by Mestre et al. in previous studies.[37] Another hypothesis is a salt segregation during the first steps of the synthesis (concretely during the drying of solution), which broke the solution's homogeneity in the ion spatial distribution. This last effect could be responsible for avoiding the suitable contact among ions, delaying the crystallization of the spinel. The problem seems to be related with the aluminium ion, which when it is involved in a SCS reaction, impedes a full crystallization in all previously studied systems.[33,37] This last conclusion will be studied in future research because of the lack of information about this concrete phenomenon.

Furnace temperature effect acted in a different way as the composition did. In all studied cases, the trend was that the higher the temperature, the more crystalline the product. Thus, this variable can be considered an important candidate to control some crystal parameters in addition to composition. The most immediate hypothesis is a crystal growth during the 20 minutes that the sample remains at fixed temperature inside the furnace. However, according to Mukasyan et al.[28] the increase of T_0 leads to an increase in the maximum combustion temperature (T_m), because a reduction of water molecules attached to the nitrates reagents when the redox reaction starts. The increase in T_m is the phenomenon that justifies the direct influence of T_0 versus crystallinity since it favors the rearrangement of ions and the development of a better-crystallized spinel structure. This effect was explained in self-propagating high-temperature

synthesis (SHS) but, by means of this research, it has been corroborated that it is also applicable in the concrete of reactions that take place in volume combustion synthesis conditions (VCS).

Furthermore, furnace temperature showed another interesting effect in the (Ni, Co)(Cr, Al)$_2$O$_4$ system. The influence of an increase in T_0 is different depending on the crystallinity degree obtained at the lowest T_0 (which is a function of composition). In the sample with a well-defined structure ($\Psi = 0.0$, $NiCr_2O_4$), an increase in T_0 subtly favors a crystallinity increase. At the same time, in systems with a low crystallinity ($\Psi = 1.0$, $CoAl_2O_4$), as composition does not favor ion rearrangement, neither a furnace temperature increase does. Nevertheless, in the intermediate range ($0.2 \leq \Psi \leq 0.8$.), T_0 is a key factor that allows the ionic rearrangement, improving crystallinity in a very effective way. This phenomenon can be clearly observed at $\Psi = 0.4$ where furnace temperature reaches its maximum influence. Therefore, composition and T_0 are complementary parameters to consider controlling pigment's crystallinity.

Crystallite size calculated from diffraction patterns by Rietveld refinement ($1.11 \leq Rwp \leq 2.56$ and $1.05 \leq GOF \leq 1.39$)[38], showed a sigmoidal trend, which was a function of composition and T_0 (Fig. 6). Crystallite size decreased considerably as Ψ augmented, regardless of furnace temperature. This fact meant that a Co^{2+} and Al^{3+} enrichment produces a negative effect on crystallite growth, more pronounced when $0.2 \leq \Psi \leq 0.8$. Regarding furnace temperature effect, higher values of T_0 clearly favors crystallite growth it in nearly all composition range. However, as previously said, the effect was more marked in the middle range of compositions. By contrast, furnace temperature effect is negligible when a low-crystallinity system is being synthesized ($\Psi = 1.0$).

An exceedingly high T_m causes a significant growth of the crystallite size and, in some compositions, the grain size. Therefore, controlling furnace temperature, which is directly related, can be considered one important research direction in order to define the resulting powder characteristics.

Considering all phenomena observed whether in SEM, specific surface and DRX studies, some correlation can be inferred. Certain relation between grain size and crystallite size was observed

because the crystallite size decreased as the grain size also did. And the effect of furnace temperature was also evidenced in both types of analyses, contributing to improve crystallite size and grain size at the same time.

Lattice parameters were also influenced by composition, but no effect of furnace temperature was observed in the data (Fig. 7). The general trend of lattice parameters followed the theoretical one calculated with Vegard's law from the values correspondent to extreme spinels. This values were obtained from the International Centre of Diffraction Data for $NiCr_2O_4$ and $CoAl_2O_4$ spinels, 8.315Å[39] and 8.060 Å[40] respectively. In fact, lattice parameter evolved according to the progressive decrease in the size of the ions in octahedral position, since Cr^{3+} (0.62 Å) presented a greater ionic radius than Al^{3+} (0.54 Å).[41] Ions in tetrahedral position does not seem to affect the trend because of their similar ionic radius. Consequently, the effect of ions in octahedral position appeared to be responsible of the lattice parameter evolution due to their higher ion size difference.

Thermal analyses were carried out with samples of extreme spinels to study the thermal behavior of the as-formed pigments in order to corroborate the results obtained by DRX, in which all structures developed were of spinel-type. Well-crystallized spinel type pigments, as $NiCr_2O_4$ was, presented no thermal events to stand out (Fig. 8). However, in the case of the low crystallinity spinel $CoAl_2O_4$ some phenomena were observed. This sample experimented three characteristic mass losses during the heating process,[42] as a result of different phenomena which had taken place during SCS reaction and the following wet-milling process. Firstly, at T ≈100ºC approximately, the loss observed is caused by two simultaneous processes. On one hand, a loss of water vapor can occur, indicative of a hydration process (humidity and adsorbed water). On the other hand, the initial loss could be a clear indicator of the amount of residual gasification components in the obtained powders, which can be emitted at those temperatures as a result of a lower reaction effectiveness.[27,43] For a complete reaction, this characteristic loss should be practically zero as it is in the case of $NiCr_2O_4$ spinel. Secondly, at T ≈400ºC sample experiences another loss that would be related to a dehydroxylation process as a result of a

previous formation of hydroxides in the sample, concretely $Al(OH)_3$ during wet-milling process. Finally, at T≈800ºC another loss of mass is observed that would be related to the reduction of Co_3O_4 to CoO. All these events also appeared in the differential thermal analysis test. In consequence, Co-rich and Al-rich samples were no as perfectly synthesized as it was expected, but they presented some unreacted components (fuel secondary products and aluminum and cobalt oxides) with low crystallinity and particle size. These high-reactivity oxides would react during the milling process with the water, forming hydroxide-type compounds. The XRD test failed to detect these unreacted oxides mainly because of their own low crystallinity. In addition, the samples presented a very high fluorescence, which favored the increase of the diffraction pattern background, which could have masked low intensity reflections.

The fact that some unreacted components were present in Ψ=1.0 sample reinforces the evidence that aluminum-rich spinels with transition metals are difficult to synthesize by SCS,[14] because of their fast kinetics that avoids a correct rearrangement of ions in a crystalline network.

All as-synthesized samples possessed an intense color, ranging from a very pure green to a very intense blue. No heterogeneities were observed in the color of the powders, which was coherent with the absence of ion segregation in the first stages of the synthesis, specifically, the water evaporation and urea decomposition. The glazes that incorporated the pigments developed saturated colors without any kind of defects, as pinholes or bubbles as it can be observed in Fig. 9. Visually, the glazes covered a palette from a practically pure green to a deep blue, also known as Thenard's blue. Fig. 10 a shows a SEM and EDX analysis of particles present into the glaze which contains the pigment synthesized at Ψ = 1.0 and T_0 = 500 ºC. The EDX results demonstrate that particles contain cobalt. Given that the transparent frit employed to prepare the glaze was cobalt-free, the EDX confirms the survival of the pigment particles, at least partially. Obviously, a fraction of pigment particles, the ones with lowest size, could have been dissolved by the glaze.

Spectrophotometric curves of glazes evolved progressively with composition (Fig. 11). The general trend observed was that as the composition increases their content in Co^{2+} and Al^{3+} the

reflectance in the ranges of green (450<λ<550) and yellow (600<λ<650) progressively decreased because of the substitution of Ni^{2+} and Cr^{3+} in the composition. Simultaneously, an important increase of the reflectance in the intervals of blue (350<λ<450) and red (λ>650) was detected. Finally, the absorption band of Co^{2+} in tetrahedral position increases its intensity abruptly when pure spinel $CoAl_2O_4$ is synthesized. No influence of the furnace temperature was observed and that is the reason whereby only spectrophotometric curves for T_0=500ºC are showed.

Regarding the CIELab* coordinates a significant evolution with composition was observed, but no effect of T_0 was detected, as expected from the spectrophotometric curves. One of the parameters that influence color development is the particle size of the pigment inserted in the ceramic glaze. In this case, the employed milling process of the pigments was not capable to individualize the grains, generating particles that grouped a big number of grains (typically the particle size was between 5 – 20 μm, and the grains according to Fig. 2 were under 500 nm). In consequence, when pigments were added into the glaze and subjected to temperatures around 1100ºC, the differences observed in grain size are not relevant as the glaze interacts with the particles. This phenomenon would be a logical explanation for the lack of influence of T_0.

The evolution of chromatic coordinates showed that the progressive addition of Co^{2+} and Al^{3+} to the spinel provokes a darker coloration in the glaze (L* coordinate decreases progressively around 15 units) until achieving a minimum point (Ψ ≈ 0.8), after which an increase of 5 units in luminosity was produced, lightening the color (Fig. 12 a). Secondly, a* was the coordinate that experienced the strangest behavior since it maintained practically constant its value (green component stable, Fig. 12 b) as Ψ grew up to 0.8 and, suddenly, skyrocketed 10 units when the composition was free of Ni^{2+} and Cr^{3+} (Ψ = 1.0), changing to a red component. Finally, b* coordinate decreased gradually around 10 units as Ψ increased up to 0.8, nearly losing the yellow component, and at Ψ>0.8 an abrupt fall of 20 units was observed, indicating a marked increase in the blue component (Fig. 12 b). Consequently, it can be said that as Ψ ≤ 0.8, Ni^{2+} and Cr^{3+} ions were able to maintain a smooth evolution of green tones. However, after this

critical value, cobalt fully exerted its influence, provoking a change in the glaze's generated color to the typical Thenard's blue.

All the synthesized products showed a behavior similar to the industrial pigments,[44,45] manufactured through high-temperature solid-solid reactions. As a reference, an industrial $CoAl_2O_4$ pigment generates in the same glaze and experimental conditions the coordinates L* = 35.5, a* = 7.0 and b*= -21.9. The color was darker and bluer than the generated by the SCS equivalents, but the differences in particle size and morphology justify the difference. On the other hand, their spongy structure and low grain size are desired characteristics for their used in the ink-jet technology, as it would ease their milling to the submicrometer particle size interval, overcoming some of the drawbacks that traditional ceramic pigments present.

4 Conclusions

Solution combustion synthesis have been revealed as an innovative wet-chemical method to develop $Ni_{1-\Psi}Co_{\Psi}Cr_{2-2\Psi}Al_{2\Psi}O_4$ ($0 \leq \Psi \leq 1$) spinel-type pigments. Synthesis variable as composition has been evidenced as a key factor, which directly influenced the crystallinity and microstructure of the products. Furnace temperature, on the contrary, showed a weaker effect on the SCS reaction.

The as-synthesized pigments presented a spongy aspect with a very low density, which made them very easy to crush. Ni and Cr richer compositions generated products with higher crystallinity and bigger crystallite sizes, properties which were progressively decreasing as the composition evolved to higher values of Ψ. For Ψ = 1.0 the spinel has a very low crystallinity and their thermal behavior points to the presence of amorphous unreacted phases. Furnace temperature exerted a noticeable effect in the ionic rearrangement to develop the spinel structure, being in the intermediate range of Ψ were their influence was more important. In consequence, furnace temperature can be considered a complementary variable to take into account when pigment final properties must be precisely controlled.

The pigments showed a high coloring power in a transparent glaze, ranging the generated tones from practically pure greens to deep blues. Although the composition was an important variable that influenced directly the final coloring power, this characteristic was practically independent of the furnace temperature. In consequence, SCS can be considered a robust fast single-step process to develop spinel-type ceramic pigments to be used in the ink-jet technology.

Acknowledgements

The authors thank Universitat Jaume I for their support for the development of this research (Project Nr. P11B2015-04).

Bibliography

1. R. A. Eppler, "Colorants for ceramics", Kirk-Othmer Encyclopedia of Chemical Technology, Wiley-Interscience, New York, Vol. 6, 877–892, 1992.

2. R. A. Eppler, "Selecting Ceramic Pigments," *Am. Ceram. Soc. Bull.*, **66** (11), 1600-1604 (1987).

3. M. Dondi, M. Blosi, D. Gardini, C. Zanelli, and P. Zannini, "Ink Technology for Digital Decoration of Ceramic Tiles: An Overview," Proceedings of the 14th World Congress on Ceramic Tile Quality, Castellón, Spain, February 17-18th, 2014.

4. I. Hutchings, "Ink-jet Printing for the Decoration of Ceramic Tiles: Technology and Opportunities," Proceedings of the 12th World Congress on Ceramic Tile Quality, Castellón, Spain, February 13-14th, 2010.

5. A. Atkinson, J. Doorbar, A. Hudd, D.L. Segal, and A. White, "Continuous Ink-jet Printing Using Sol-gel "Ceramic" Inks," *J. Sol-Gel Sci. Technol.*, **8**, 1093-1097 (1997). doi:10.1007/BF02436989.

6. I. V. Pishch and E. V. Radion, "Use of the Precipitation Method in the Synthesis of Ceramic Pigments," *Glass Ceram.*, **62**, 189-191 (2005). doi:10.1007/s10717-005-0069-2.

7. I. V. Pishch and E. V. Radion, "A Pigment Based on Coprecipitated Iron (III) and Nickel (III) Hydroxides," *Glass Ceram.*, **53**, 178–179 (1996). doi:10.1007/BF01166033.

8. S. Sanjabi, and A. Obeydavi, "Synthesis and Characterization of Nanocrystalline $MgAl_2O_4$ Spinel Via Modified Sol–gel Method, *J. Alloy Compd.*, **645**, 535–540 (2015). doi:10.1016/j.jallcom.2015.05.107.

9. P. Escribano, M. Marchala, M. L. Sanjuán, P. Alonso-Gutiérrez, B. Julián et al., "Low-temperature Synthesis of $SrAl_2O_4$ by a Modified Sol–gel Route: XRD and Raman Characterization," *J. of Solid State Chem.*, **178**, 1978–1987 (2005). doi:10.1016/j.jssc.2005.04.001.

10. L. K. C. de Souza, J. R. Zamian, G. N. da Rocha, L. E. B. Soledade, I. M. G. dos Santos et al. "Blue Pigments Based on $Co_xZn_{1-x}Al_2O_4$ Spinels Synthesized by the Polymeric Precursor Method," *Dyes Pigments*, **81**, 187–192 (2009). doi:10.1016/j.dyepig.2008.09.017.

11. L. Gama, M. A. Ribeiro, B. S. Barros, R. H. A. Kiminami, I. T. Weber, et al., "Synthesis and Characterization of the $NiAl_2O_4$, $CoAl_2O_4$ and $ZnAl_2O_4$ Spinels by the Polymeric Precursors Method," *J. Alloy Compd.*, **483**, 453-455 (2009). doi:10.1016/j.jallcom.2008.08.111.

12. N. Ouahdi, S. Guillemet, B. Durand, R. El Ouatib, L. Er Rakho, et al., "Synthesis of $CoAl_2O_4$ by Double Decomposition Reaction Between $LiAlO_2$ and Molten $KCoCl_3$," *J. Eur. Ceram. Soc.*, **28**, 1987-1994 (2008). doi:10.1016/j.jeurceramsoc.2007.12.035.

13. S. T. Aruna, "Solution Combustion Synthesis-An Overview", Chapt. 16, 206-221, Combustion Synthesis: Novel Routes to Novel Materials, Maximilian Lackner ed., Bentham Science Publishers, Viena University of Technology, Austria, 2010. doi: 10.2174/97816080515571100101.

14. K. C. Patil, M. S. Hedge, T. Rattan, and S. T. Aruna, *Chemistry of nanocrystalline oxide materials: Combustion synthesis, properties and applications*. World Scientific Publishing, Singapore, 2008.

15. M. C. Gardey Merino, A. L. Estrella, M. E. Rodriguez, L. Acuña, M. S. Lassa et al., "Combustion Syntheses of $CoAl_2O_4$ Powders Using Different Fuels," *Procedia Mater. Sci.*, **8**, 519-525 (2015). doi: 10.1016/j.mspro.2015.04.104.

16. K. Christine Stella and A. Samson Nesaraj, "Effect of Fuels on the Combustion Synthesis of $NiAl_2O_4$ Spinel Particles," *Iran. J. of Mater. Sci. Eng.*, **7** [2], 36-44 (2010).

17. S. T. Aruna and K. C. Patil, "Synthesis and Properties of Nanosized Titania," *J. Mater. Synth. Proces.*, **4**, 175-176 (1996).

18. R. Ianoş, A. Tăculescu, C. Păcurariu, and I. Lazău, "Solution Combustion Synthesis and Characterization of Magnetite, Fe_3O_4, Nanopowders," *J. Am. Ceram. Soc.*, **95**, 2236-2240 (2012). doi: 10.1111/j.1551-2916.2012.05159.x.

19. J. J. Kingsley and K. C. Patil, "A Novel Combustion Process for the Synthesis of Fine Particle α-Alumina and Related Oxide Materials," *Mater. Lett.*, **6**, 427-432 (1988). doi:10.1016/0167-577X(88)90045-6.

20. S. S. Manoharan and K. C. Patil, "Combustion Synthesis of Metal Chromite Powders," *J. Am. Ceram. Soc.*, **75**, 1012-1015 (1992). doi: 10.1111/j.1151-2916.1992.tb04177.x.

21. K. Suresh, N. R. S. Kumar, and K. C. Patil, "A Novel Combustion Synthesis of Spinel Ferrites, Orthoferrites and Garnets," *Adv. Mater.*, **3**, 148-150 (1991). doi: 10.1002/adma.19910030306.

22. S.T. Aruna, A.S. Mukasyan, "Combustion Synthesis and Nanomaterials," *Curr. Opin. Solid St. M.,* **12,** 44–50 (2008). doi: 10.1016/j.cossms.2008.12.002

23. R. Ianoș, P. Barvinschi, "Characterization of $Mg_{1-x}Ni_xAl_2O_4$ Solid Solutions Prepared by Combustion Synthesis," *J. Eur. Ceram. Soc.,* **31**, 739–743 (2011). doi: 10.1016/j.jeurceramsoc.2010.12.011

24 R. Ianoș, R. Lazău, P. Barvinschi, "Synthesis of $Mg_{1-x}Co_xAl_2O_4$ Blue Pigments Via Combustion Route," *Adv. Powder Technol.*, **22**, 396–400 (2011). doi: 10.1016/j.apt.2010.06.006

25. I. Lazău, C. Păcurariu, Z. Ecsedi, R. Ianoș, Peculiarities of Ceramic Powders Synthesis Using the Combustion Method. *Rev. Roum. Chim.*, **50**, 919–927 (2005).

26. Z. Tian, H. Yu, Z. Wang, "Combustion Synthesis and Characterization of Nanocrystalline $LaAlO_3$ Powders," *Mater. Chem. Phys.*, **106**, 126–129 (2007). doi: 10.1016/j.matchemphys.2007.05.027

27. R. G. Ianos, *Temperature and atmosphere influence during combustion synthesis of metal oxide (nano)powders*, PhD thesis, Politehnica University of Timișoara, Faculty of Industrial Chemistry and Environmental Engineering, 2015.

28. A. S. Mukasyan, P. Epstein, and P. Dinka, "Solution Combustion Synthesis of Nanomaterials," *P. Combust. Inst.*, **31**, 1789–1795 (2007). doi:10.1016/j.proci.2006.07.052.

29. K. C. Patil and T. Mimani, "Solution Combustion Synthesis of Nanoscale Oxides and Their Composites", *Mater. Phys. Mech.*, **4**, 134-137 (2001).

30. A. G. Merzhanov, *Combustion: New manifestation of an ancient process*, Rao CNR eds., Chemistry of Advanced Materials, Blackwell Scientific, Oxford, 19-39, 1993.

31. J. J. Kingsley, K. Suresh, and K. C. Patil, "Combustion Synthesis of Fine-particle Metal Aluminates," *J. Mater. Sci.*, **25** (2), 1305-1312 (1990).

32. Color Pigments Manufacturers Association (CPMA), "Classification and chemical descriptions of the complex inorganic color pigments", 4th ed., Alexandria (VA), 2013.

33. W. Wen and J. M. Wu, "Nanomaterials Via Solution Combustion Synthesis: A Step Nearer to Controllability," *RSC Adv*. **4**, 58090-58100 (2014). doi: 10.1039/c4ra10145f.

34. F. J. Torres, E. Ruiz de Sola, and J. Alarcón, "Effect of Some Additives on the Development of Spinel-based Glass-ceramic Glazes for Floor-tiles," *J. of Non-Cryst. Solids*, **351**, 2453–2461 (2005). doi: 10.1016/j.jnoncrysol.2005.06.027.

35. M.P. Gómez-Tena, J. Gilabert, J. Toledo, E. Zumaquero, and C. Machí, "Relationship Between the Specific Surface Area Parameters Determined Using Different Analytical Techniques", Qualicer 2014: XIII World congress on ceramic tiles. Castellón: Cámara Oficial de Comercio, Industria y Navegación, 2014.

36. S. Mestre, M. D. Palacios, and P. Agut, "Solution Combustion Synthesis of (Co,Fe)Cr_2O_4 Pigments," *J. Eur. Ceram. Soc.*, **32** (9), 1995–1999 (2012). doi:10.1016/j.jeurceramsoc.2011.11.044

37. J. Gilabert, M. D. Palacios, V. Sanz, and S. Mestre, "Characteristics Reproducibility of (Fe, Co)(Cr, Al)$_2O_4$ Pigments Obtained by Solution Combustion Synthesis," *Ceram. Int.*, **42** 12880-12887 (2016). doi:10.1016/j.ceramint.2016.05.054

38. B.H. Toby, "R factors in Rietveld analysis: How good is good enough?," *Powder Diffr.*, **21** 67-70 (2006). doi: 10.1154/1.2179804

39. International Center for Diffraction Data (ICDD) PDF-4+ file, ICDD 04-006-0279.

40. International Center for Diffraction Data (ICDD) PDF-4+ file, ICDD 04-008-3316.

41. D. R. Lide ed., "CRC handbook of chemistry and physics", 74th ed., CRC Press, Boca Raton, 1993.

42. T. Hatakeyama, L. Zhenhai eds., "Handbook of thermal analysis", John Wiley & sons, Reimp, Chichester, 2000.

43. S. Désilets, P. Brousseau, D. Chamberland, S. Singh. H. Feng, R. Turcotte, K. Armstrong, J. Anderson, "Analyses of the thermal decomposition of urea nitrate at high temperature," Thermochimica Acta, 521, 59-65 (2011). doi: 10.1016/j.tca.2011.04.004

44. J.M. Rincón, J. Carda, and J. Alarcón, *Nuevos productos y tecnologías de esmaltes y pigmentos cerámicos (New products and technologies of glazes and ceramic pigments)*. Faenza Editrice Ibérica, Castellón, 1992.

45. Escribano P, Carda JB, Cordoncillo E. *Esmaltes y pigmentos cerámicos (Glazes and ceramic pigments)*. Faenza Editrice Ibérica, Castellón, 2001.

Figure captions

Figure 1 Images showing spinel spongy aspect evolution at three different composition steps (T_0 = 500 ºC)

Figure 2 Micrographies obtained on the as-synthesized pigments with different compositions (Ψ=0.0, Ψ=0.4 and Ψ=1.0) and furnace temperatures (T=400ºC and T=600ºC)

Figure 3 Chemical analysis by EDX of selected pigments with different compositions and furnace temperatures

Figure 4. DRX phase identification for all composition range of $Ni_{1-\Psi}Co_{\Psi}Cr_{2-2\Psi}Al_{2\Psi}O_4$ ($0 \leq \Psi \leq 1$) samples synthesized at T_0 = 500ºC (○ spinel)

Figure 5. Diffraction patterns around I_{100} of spinel structure of all synthesized pigments $Ni_{1-\Psi}Co_{\Psi}Cr_{2-2\Psi}Al_{2\Psi}O_4$ ($0 \leq \Psi \leq 1$) obtained at three different furnace temperatures

Figure 6 Crystallite size calculated by Rietveld refinement versus composition and furnace temperature

Figure 7 Lattice parameters with Vegard's law prediction versus composition and furnace temperature

Figure 8 Simultaneous thermal analyses of samples Ψ=0.0 and Ψ=1.0: a) Thermogravimetric analyses, b) Differential thermal analyses

Figure 9 Example of glazed samples at T_0 = 500ºC showing saturated colors with no defects on the surface

Figure 10. SEM analysis of particles present in the glaze which contains the Ψ=1.0 pigment: a) SEM micrography and b) EDX analysis of the pigment particles

Figure 11 Spectrophotometric curves of the glazes which incorporated the pigments synthesized at T_0 = 500ºC

Figure 12 CIELab* coordinates versus composition and furnace temperature, a) L* coordinate and b) a* and b* coordinates

Tables and table captions

Table I Composition of initial solutions

Ref.	Ψ	Urea (g)	$Ni(NO_3)_2 \cdot 6H_2O$ (g)	$Co(NO_3)_2 \cdot 6H_2O$ (g)	$Cr(NO_3)_3 \cdot 9H_2O$ (g)	$Al(NO_3)_3 \cdot 9H_2O$ (g)	H_2O (mL)
S1	0.0	24.0	17.45	---	48.0	---	50
S2	0.2		13.96	3.49	38.4	9.00	
S3	0.4		10.47	6.98	28.8	18.00	
S4	0.6		6.98	10.48	19.2	27.01	
S5	0.8		3.49	13.97	9.6	36.01	
S6	1.0		---	17.46	---	45.01	

Table II Specific surface area values (m^2/g) for tested samples

Composition	Furnace temperature	
	400ºC	600ºC
Ψ=0.0	13	10
Ψ=0.4	25	21
Ψ=1.0	227	167

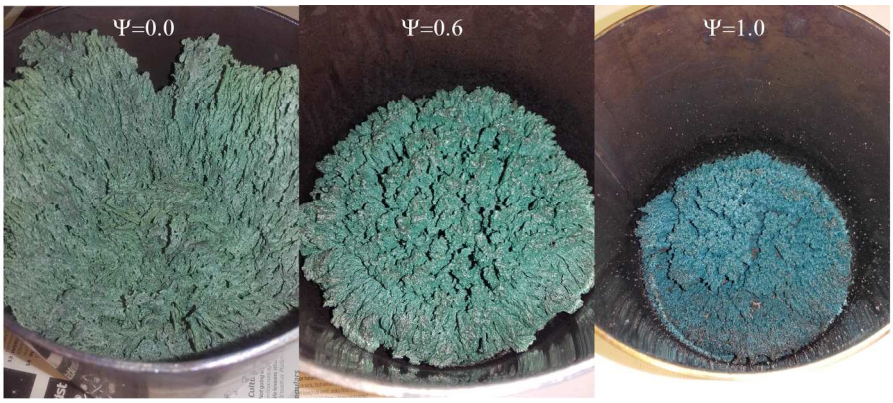

Figure 1. Images showing spinel spongy aspect evolution at three different composition steps (T_0 = 500 ºC)

169x66mm (300 x 300 DPI)

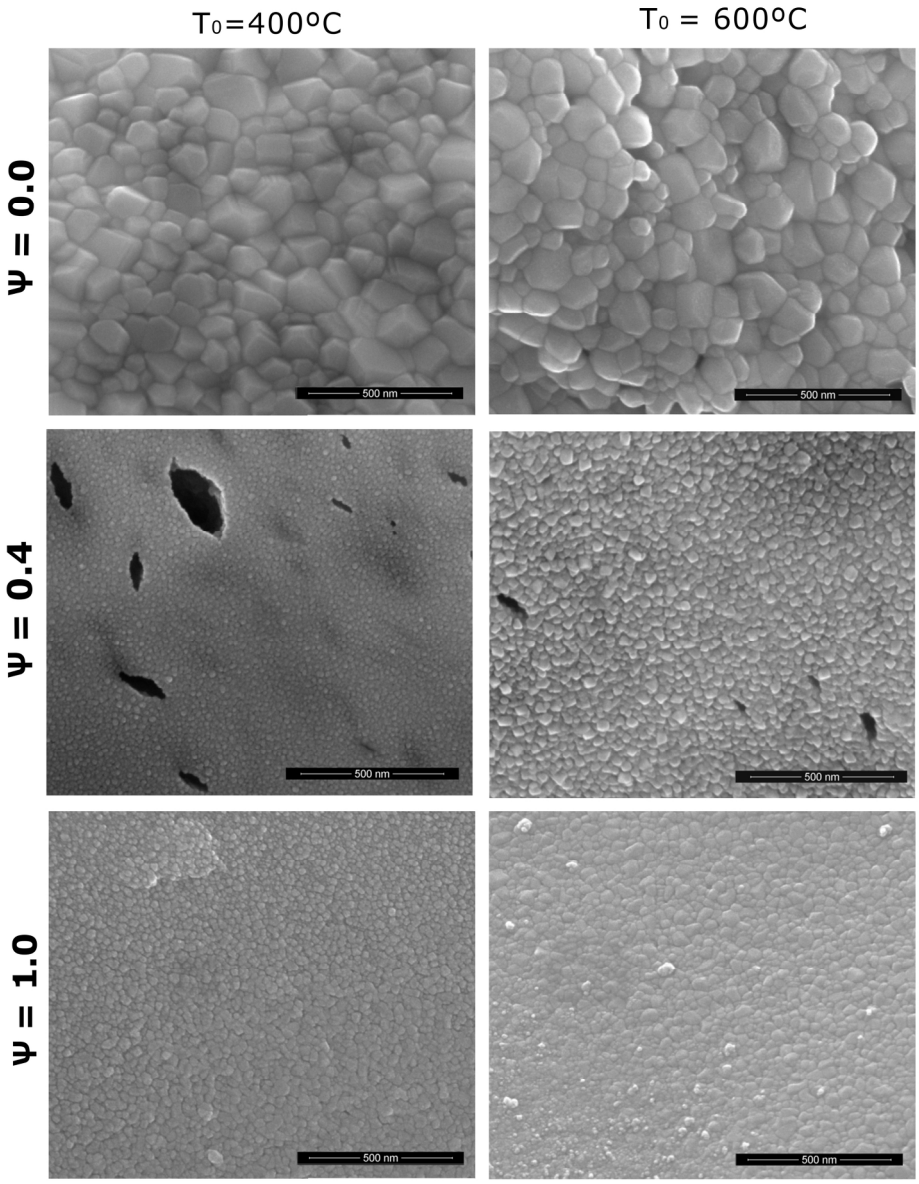

Figure 2. Micrographies obtained on the as-synthesized pigments with different compositions (ψ=0.0, ψ=0.4 and ψ=1.0) and furnace temperatures (T_0=400ºC and T_0=600ºC)

180x231mm (300 x 300 DPI)

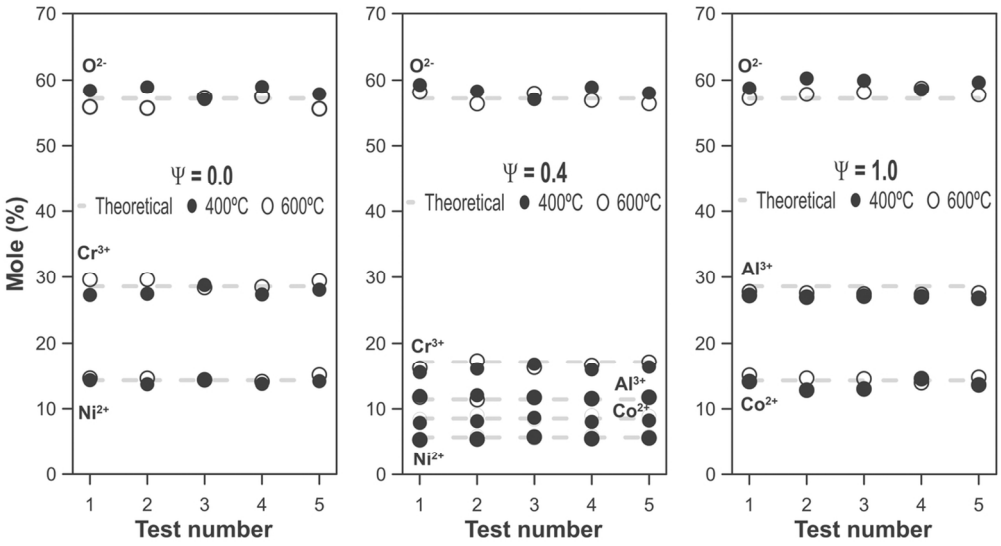

Figure 3. Chemical analysis by EDX of selected pigments with different compositions and furnace temperatures

54x29mm (600 x 600 DPI)

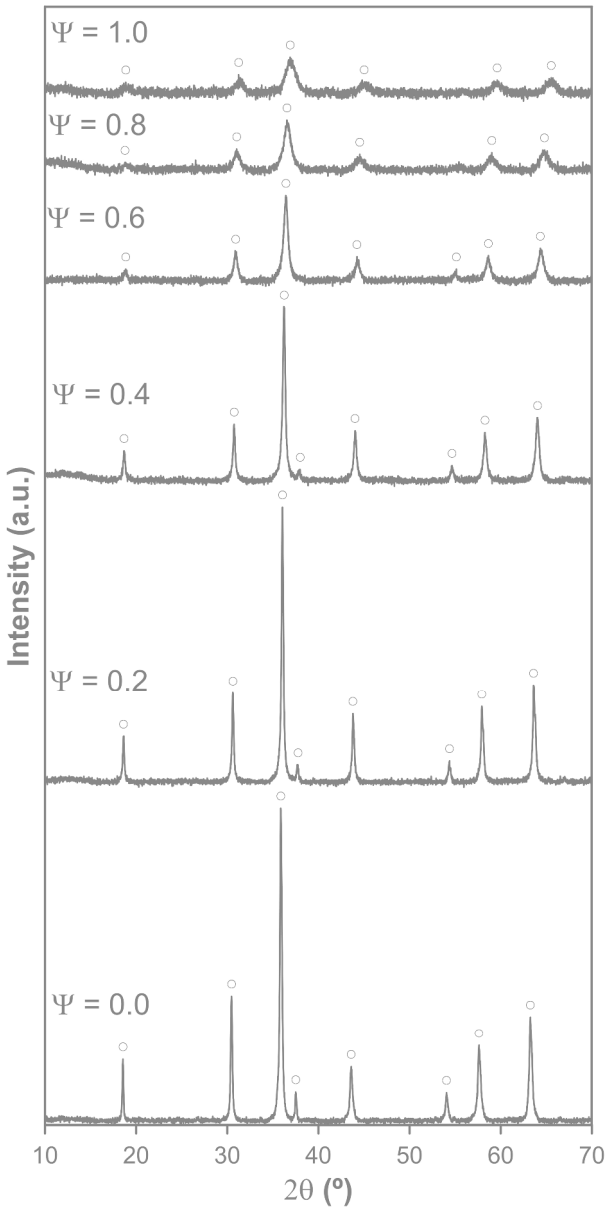

Figure 4. XRD phase identification for all composition range of $Ni_{1-\psi}Co_{\psi}Cr_{2-2\psi}Al_{2\psi}O_4$ ($0 \leq \Psi \leq 1$) samples synthesized at T_0 = 500ºC (O spinel)

142x284mm (600 x 600 DPI)

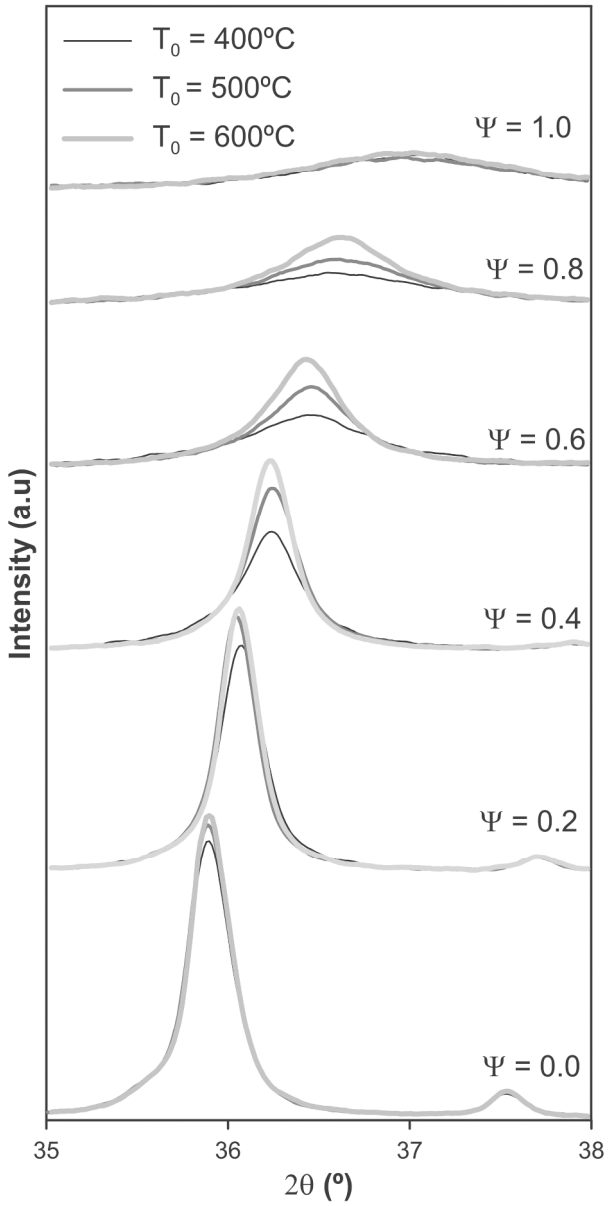

Figure 5. Diffraction patterns around I100 of spinel structure of all synthesized pigments $Ni_{1-\psi}Co_{\psi}Cr_{2-2\psi}Al_{2\psi}O_4$ ($0 \leq \Psi \leq 1$) obtained at three different furnace temperatures

101x202mm (600 x 600 DPI)

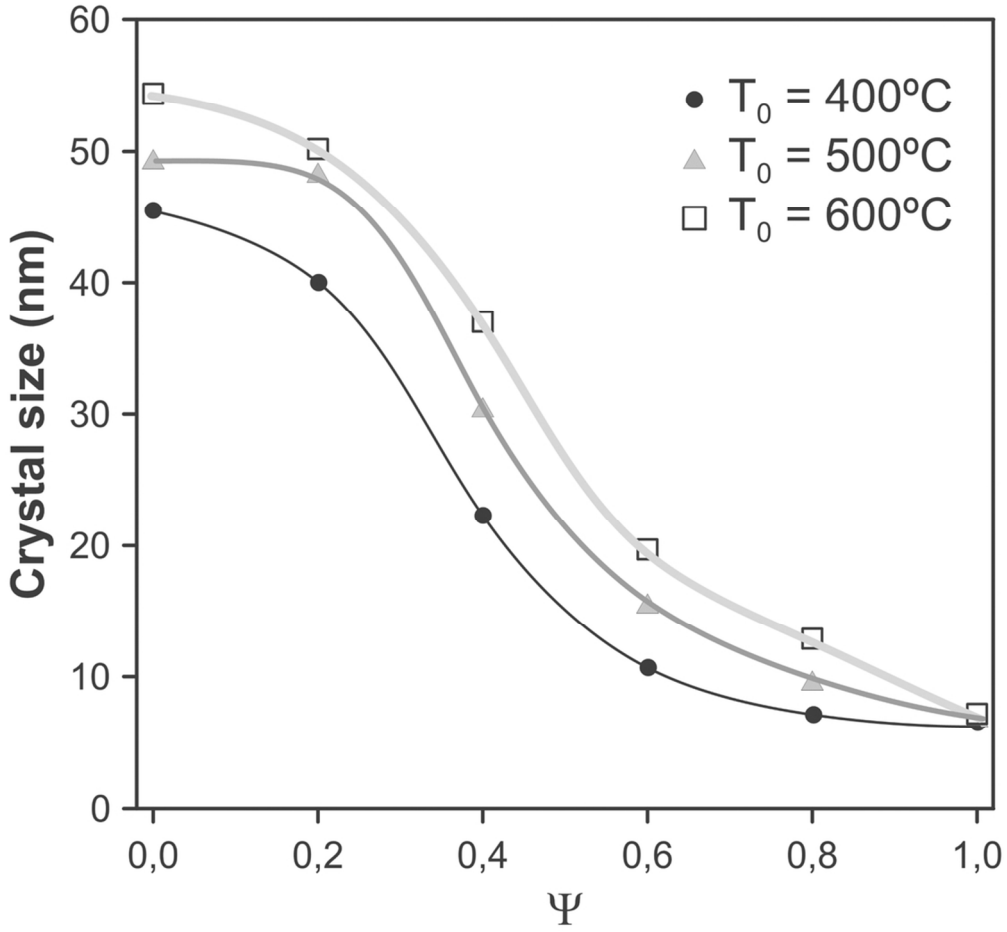

Figure 6. Crystallite size calculated by Rietveld refinement versus composition and furnace temperature

47x44mm (600 x 600 DPI)

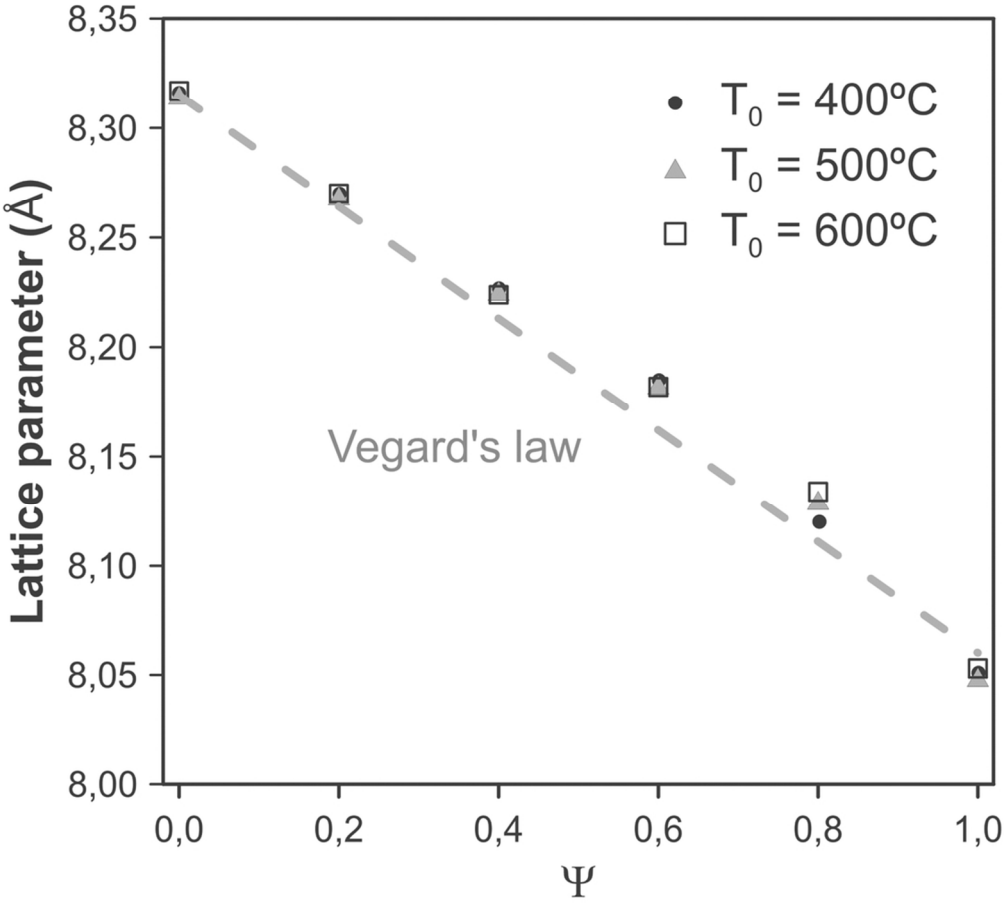

Figure 7 Lattice parameters with Vegard's law prediction versus composition and furnace temperature

46x41mm (600 x 600 DPI)

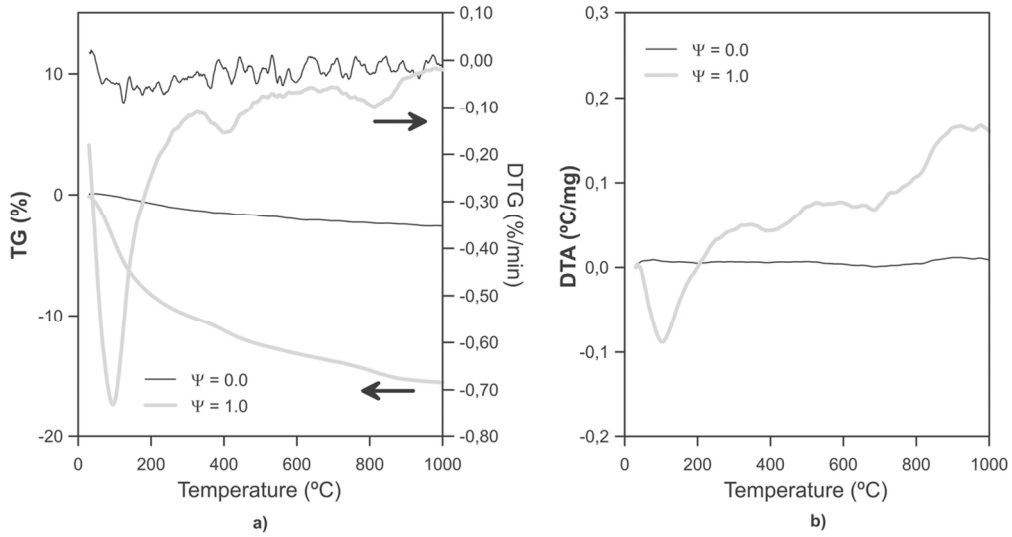

Figure 8 Simultaneous thermal analyses of samples ψ=0.0 and ψ=1.0: a) Thermogravimetric analyses, b) Differential thermal analyses

53x28mm (600 x 600 DPI)

Figure 9 Example of glazed samples at T_0 = 500ºC showing saturated colors with no defects on the surface

169x196mm (300 x 300 DPI)

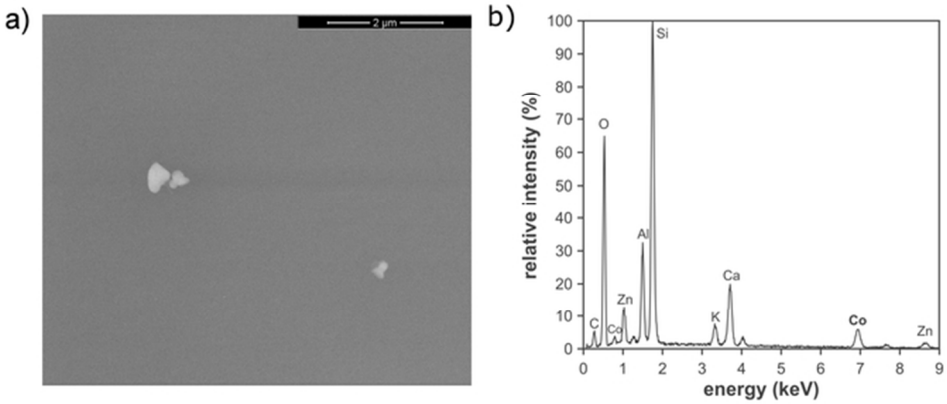

Figure 10. SEM analysis of particles present in the glaze which contains the ψ=1.0 pigment: a) SEM micrography and b) EDX analysis of the pigment particles

59x25mm (300 x 300 DPI)

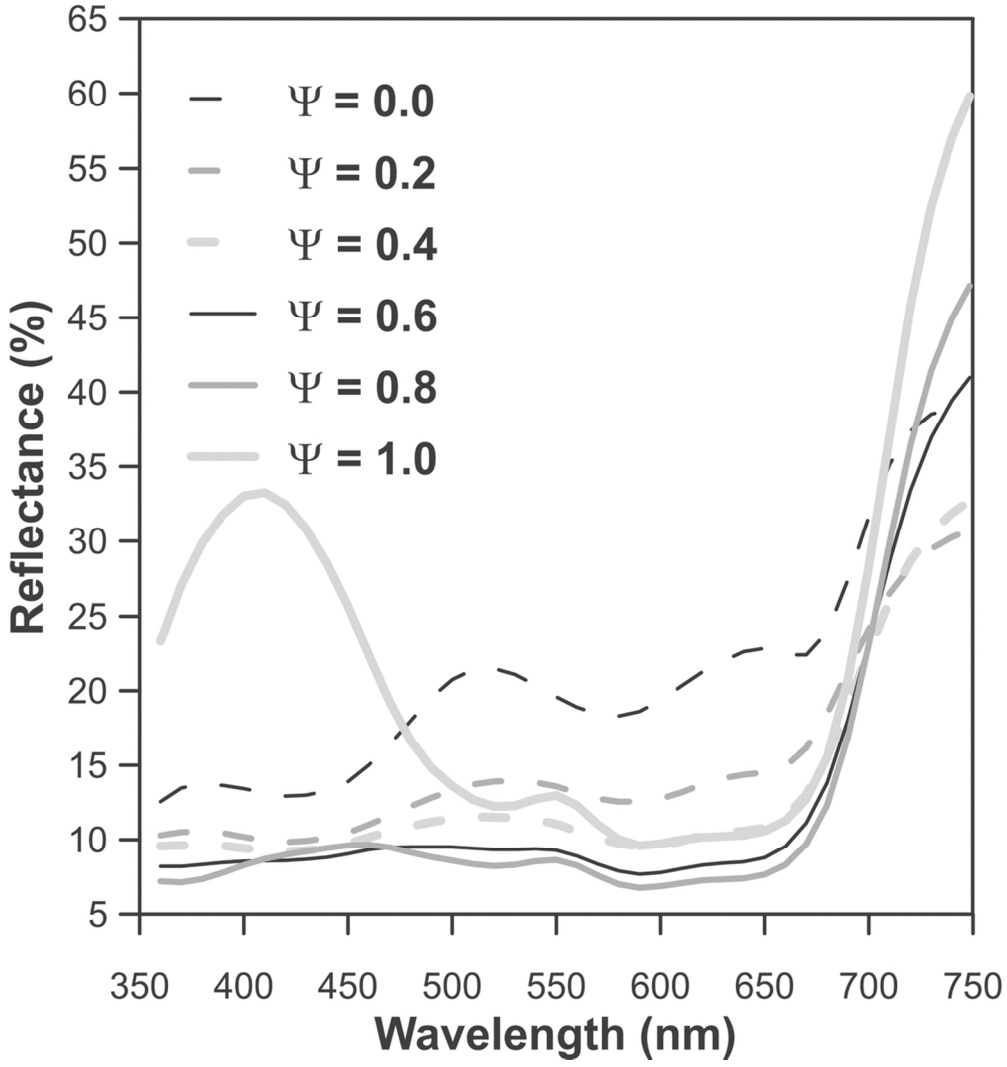

Figure 11. Spectrophotometric curves of the glazes which incorporated the pigments synthesized at T_0 = 500ºC

53x57mm (600 x 600 DPI)

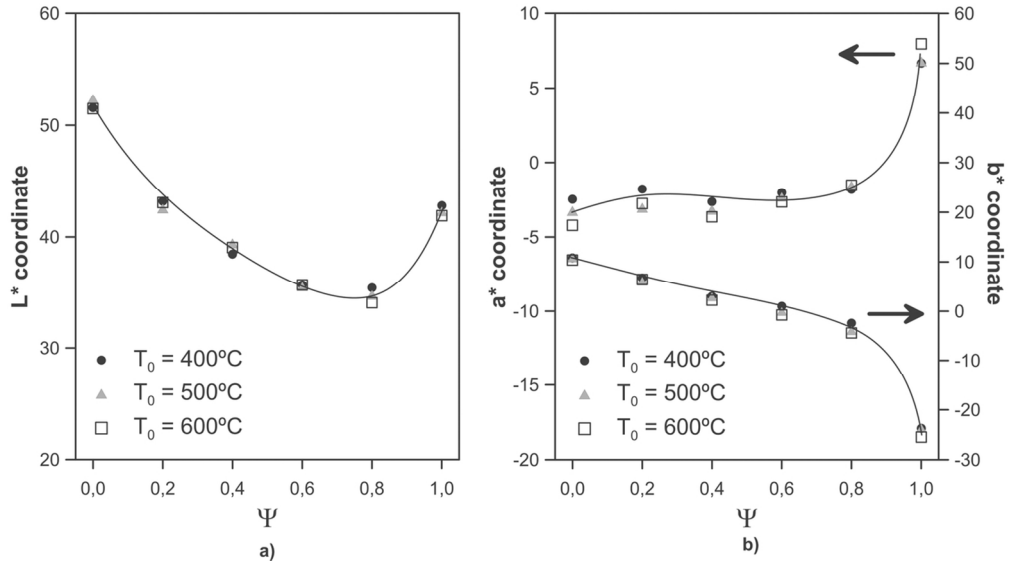

Figure 12. CIELab* coordinates versus composition and furnace temperature, a) L* coordinate and b) a* and b* coordinates

56x31mm (600 x 600 DPI)